LncRNA MIR497HG suppresses bladder cancer progression through disrupting the crosstalk between Hippo/Yap and TGF-β/Smad signaling

Changshui Zhuang
Peking University
Ying Liu
Peking University
Chaobo Yuan
Peking University
Shengqiang Fu
Peking University
Weifeng Yang
Peking University
Jingwen Luo
Peking University
Chengle Zhuang (clzhuang@hsc.pku.edu.cn)
Peking University https://orcid.org/0000-0001-9145-1146

Research

Keywords: Bladder cancer, MIR497HG, miR-497, miR-195, Yap, TGF-β

Posted Date: August 31st, 2020

DOI: https://doi.org/10.21203/rs.3.rs-64839/v1

Abstract

Objectives

A subclass of long non-coding RNAs (lncRNAs), categorized as miRNA-host gene lncRNAs (lnc-miRHGs), is processed to produce miRNAs and involve in cancer progression. This work aimed to investigate the influence and the molecular mechanisms of lnc-miRHGs MIR497HG in bladder cancer (BCa).

Materials and methods

The miR-497 and miR-195 were derived from MIR497HG. Cell proliferation, migration and invasion assays were used to measure the function of MIR497HG, miR-497 and miR-195 in BCa. Bioinformatics, RT-qPCR, western blot, luciferase reporter assay, ChIP, and so on, were used to reveal the upstream and downstream mechanisms of MIR497HG in BCa.

Results

We identified that lnc-miRHG MIR497HG and two harbored miRNAs, miR-497 and miR-195, were downregulated in BCa by analyzing TCGA and our dataset. MIR497HG overexpression inhibited BCa cell proliferation, migration and invasion *in vitro*. MiR-497/miR-195 inhibitor rescued significantly the inhibiton effects of overexpression of MIR497HG in BCa. Mechanistically, miR-497 and miR-195 coordinately suppressed multiple key components in Hippo/Yap and TGF-β signaling, and particularly attenuated the interaction between Yap and Smad3. In addition, E2F4 was proved to be critical for silencing MIR497HG transcription in BCa cells.

Conclusions

We propose for the first time that MIR497HG suppressed BCa progression and its upstream and downstream mechanisms. Blocking the pathological process may be a potential strategy for the treatment of BCa.

1. Introduction

Bladder cancer (BCa) is one of the most prevalent epithelial malignancy worldwide [1]. Most of diagnosed patients have non–muscle-invasive bladder cancer (NMIBC) confined to the mucosa or lamina propria and approximately 25% have muscle-invasive (MIBC) that invade the detrusor muscle [2, 3]. MIBC is more aggressive and have a worse prognosis [2, 4]. Existing therapies for MIBC have not changed mortality rates over the past years [4]. Genome and transcriptome profiling studies have revealed considerable differences in the molecular and genetic features of bladder cancer cells, such as mutations, copy

number, and gene epigenetic alterations, determining tumor heterogeneity and therapeutic resistance [2, 5, 6]. However, non-genetic or epigenetic mechanisms in BCa remain elusive.

Non-coding RNAs (ncRNAs), especially long non-coding RNAs (lncRNAs, > 200nt) and microRNAs (miRNAs, 20-22nt), are critical for epigenetic regulation [7, 8]. Recent studies have reported certain lncRNAs, are referred as miRNA-host gene, and acquire functionality by serving as the precursor to microRNAs capable of regulatory role [9–11]. For example, MIR100HG-derived miR-100 and miR-125b induce cetuximab resistance via augmenting Wnt signaling [12]. MiR-675 derives from lncRNA-H19, inhibites cell proliferation in response to cellular stress or oncogenic signals [13]. MiR-17 ~ 92 cluster miRNAs encoded by MIR17HG downregulates TGF-β and STAT3 signaling in feingold syndrome mouse models [14]. LncRNA MIR497HG and derived miR-497 ~ 195 cluster are downregulated in BCa [15, 16]. Furthermore, miR-195 and miR-497 expression are repressed and they function as tumor suppressors in various types of human cancer including breast cancer [17], lung cancer [18], colorectal cancer [19] and hepatocellular carcinoma [20]. However, the impact of these lncRNAs or derived miRNAs in BCa progression are largely unknown.

Many signaling pathways such as JAK-STAT, NF-KB, mTOR and MAPK have been reported to affect the survival of BCa [21]. Evolutionarily conserved Hippo pathway has been shown to paly crtical roles during BCa progression and tumorigenesis [22]. The Hippo pathway regulates cell proliferation and migration via the transcriptional coactivator Yes-associated protein (YAP) [23]. YAP is highly expressed and acts as oncogenes in BCa [24, 25]. Transforming growth factor beta (TGF-β) complex, a serine/threonine kinase complex, binds to TGF-β receptors and further activates different downstream substrates and regulatory proteins, mainly the SMAD, inducing transcriptions of different target genes involving in cell proliferation, differentiation, and so on [26]. Besides, activation of the TGF-β/Smad signaling pathway often correlates with the malignancy of lots of human cancer, including BCa [27].

Here we report that MIR497HG plays anti-tumorigenic roles in BCa. We found that miR-497, miR-195 and their host gene MIR497HG were down-expressed in BCa tissues and cell lines. MiR-497 and miR-195 synergistically targeted YAP and SMAD3 and their downstream genes, and decreased the formation of a YAP-SMAD complex [28]. We also identified that E2F4 is a critical transcriptional suppressor of MIR497HG. Our findings uncover an ncRNAs-mediated epigenetic mechanism to block the crosstalk between Hippo/Yap and TGFβ/Smad signaling. It may contribute to search for effective personalized targeted therapies to treat BCa.

2. Materials And Methods

2.1 Cell culture

Normal human immortalized urothelial cell line SV-HUC-1 and the human BCa cell lines T24, 5637, RT4, UM-UC-3, SW780 and TCCSUP were purchased from the American Type Culture Collection (ATCC, Manassas, VA). T24, 5637 and SW780 were cultured in RPMI-1640 medium. UM-UC-3 and TCCSUP were

cultured in DMEM. RT4 was cultured in Mcoy's 5a, and SV-HUC-1 was cultured in F-12K medium. 10% fetal bovine serum (FBS; Biological Industries, Beit Haemek, Israel) and 1% penicillin/streptomycin (GIBCO, Gaithersburg, MD, USA) were added to get complete growth medium.

2.2 BCa specimens

All BCa samples were collected from the Peking University Shenzhen Hospital and Shenzhen University Nanshan Hospital. The study was approved by the Ethics Committee of Shenzhen University Nanshan Hospital with written informed consent obtained from all patients. The pathological status of the specimens was provided by the board-certified pathologist.

2.3 Western blot

Protein extracts were prepared in RIPA Lysis Buffer (#P0013B; Beyotime), supplemented with PMSF, protease inhibitor and phosphatase inhibitor cocktail. Protein concentrations were determinated using Bicinchoninic Acid Kit (Sigma-Aldrich) according to the manufacturer's protocol. Cell lysates were resolved by SDS-PAGE and transferred onto PVDF membranes. Membranes were blocked for 1 hour with 5% non-fat milk in TBST (Trisbuffered saline containing 0.1% Tween 20) and incubated overnight at 4 °C with primary antibodies and required secondary antibodies conjugated to horseradish peroxidase and developed by chemiluminescent substrates.

2.4 RT-qPCR and ChIP

Total RNA was extracted using TRIzol™ Reagent (Invitrogen) and purified using RNeasy Mini Columns (Qiagen), according to the manufacturer's protocol. For mRNA and lncRNA MIR497HG detection, cDNA was generated using SureScript™ First-Strand cDNA Synthesis Kit (genecopoeia). Quantitative PCR was then performed using the SYBR Green qPCR MasterMix (Takara). To analyze miR-195 and miR-497 expression, cDNA was synthesized by a mir-X miRNA First-Strand Synthesis Kit (Takara,Dalian, China). MiRNA expression were used mir-X miRNA qRT-PCR SYBR Kit (TOYOBO, Osaka, Japan) according to the manufacturer's instructions, with U6 as the control.

2.5 Chromatin immunoprecipitation (ChIP)

Chromatin immunoprecipitation (ChIP) assays were performed according to manufacturer's instructions using Cell Signaling Immunoprecipitation Kit (#9002). Briefly, 5637 cells were fixed paraformaldehyde and lysed in Buffer A supplemented with DTT, Protease Inhibitor Cocktail (PIC), and PMSF, and incubated on ice for 10 min. Nuclei were pelleted and resuspended in Buffer B + DTT. DNA was digested with 0.5 ul Micrococcal Nuclease. Nuclei were again pelleted, resuspended in ChIP buffer + PIC and PMSF, and incubated at 4 °C. The lysates were clarified by centrifugation and ChIP was carried out by incubating the sample with Rabbit IgG or E2F4 antibody (Abcam), followed by immobilization on protein A/G-agarose beads (Life Technologies). The chromatin was eluted from Antibody/Protein G Agarose Beads, cross-links were reversed, and DNA was purified using spin columns. The qPCR was performed using MIR497HG promoter or GAPDH primers. Ct values were normalized to input DNA. The detailed primer sequences for RT-qPCR and ChIP assays are listed in supplementary Table S1.

2.6 Cell Counting Kit-8 (CCK-8) assay

Cells were cultured in 96-well plates at a concentration of 3×10^3 cells per well. After treatment, 10 μl CCK-8 reagent (Dojindo, Kumamoto, Kyushu, Japan) was added to each well to react for 0.5 h. The absorbance was measured at 450 nm using a microplate reader.

2.7 Colony formation assay

1000 cells/well were plated onto six-well plates, which were incubated at 37℃ and 5% CO2 until colonies were formed. After 10–15 days, colonies were fixed using 0.05% crystal violet in 4% paraformaldehyde and counted using Image J program.

2.8 Cell migration assay

Cells were seeded in six-well plate (5×10^5/per well) and incubated at 37 °C in a humidified incubator containing 5% CO2 to get 100% confluence before transfection. A clear line was created by scratching with a sterile 200 μl pipette tip. Images were taken from each well quickly. After 24 hours, pictures were taken again with the help of a digital camera system. Migration distance was calculated at the time of 0 and 24 h. Experiments were performed at least three times.

2.9 Cell invasion assay

Cells were transfected with siRNAs/plasmids for 48 h and then trypsinized and resuspended in serum-free medium. A total of 1×10^5 cells were then added to the upper chambers of the Transwell inserts (Millicell; Merck KGaA) and allowed to migrate toward the bottom of the chambers. After 24 h, the remaining cells in the upper chamber were removed, and cells on the underside were fixed in 4% paraformaldehyde for 30 min at room temperature, stained with 0.1% crystal violet for 30 min at room temperature and captured using an Olympus type light microscope sz30. Quantification of the migrated cells was performed by counting cell numbers.

2.10 Plasmids, lentiviral production and transfection

YAP1 and SMAD3 coding sequence was cloned into pCMV-HA-N expression vector (SalI/BglII and KpnI/NotI). The primer sequences used for clone are provided in supplementary Table S1. pLemiR control, pLemiR-195 or pLemiR-497 plasmid were packaged with pMDL,VSVG and pRSV-Rev into HEK-293T cells. To establish stable cell lines, the concentrated lentivirus were directly added into cancer cells and incubated at 37 °C for 48 hours before they were washed out PBS. Finally, cells were selected with 2.5 mg/mL puromycin for 4 days. For luciferase reporter assay, the 3’ UTR fragments of YAP1, SMAD3,CCND1 and BIRC5 containing the wild-type or mutant miR-497 ~ 195 cluster putative target sites were directly synthesized from GeneCreate (Wuhan, China), and cloned downstream of the Renilla luciferase cassette in psiCHECK-2 (Promega);The CTGF-luc plasmids were generated as described previously [29]. The promoter fragments of human MIR497HG were directly synthesized from GeneCreate (Wuhan, China), and cloned into pGL3-Basic vector (Promega). A site-directed mutagenesis kit (Thermo Fisher Scientific) was used to mutate the miR-497 ~ 195 cluster or E2F4 binding sites of these vectors.

The primer sequences used for the site-directed mutagenesis are provided in supplementary Table S1. All sequences were confirmed by sequencing.

The miRNA inhibitors and mimics of miR-ctrl, miR-195 and miR-497 were obtained from Ribobio (Guangzhou, China). The indicated cancer cells were transfected with 50 nM of mimic or inhibitor of miR-ctrl, miR-195 and miR-497 using Lipofectamine 3000 (Invitrogen, Carlsbad, CA, USA) according to the manufacturer's protocol. The expression levels of miR-195 and miR-497 were quantified after 48 h transfection.

2.11 Luciferase reporter assay

For 3' UTR luciferase reporter assays, miR-497 or miR-195 mimic or control mimic (Ambion) and indicated psiCHECK-2-3' UTR wild-type or mutant plasmids were co-transfected into T24 or 5637 cells cultured in 24-well plates using lipofectamine 3000 (Thermo Fisher Scientific). Renilla and firefly luciferase activities were measured with the dual-luciferase reporter assay system (Promega, Madison, WI, USA) according to the manufacturer's manual.

For luciferase reporter assay, in order to measure promoter activities, the MIR497HG promoter fragment was inserted into pGL3-basic plasmid, named pGL3-MIR497HG. Then pcDNA3.1-E2F4 expression plasmid or empty vector control and pGL3-MIR497HG or pGL3-MIR497HG-mut were co-transfected into T24 or 5637 cells cultured in 24-well plates using lipofectamine 3000 (Thermo Fisher Scientific). The firefly and Renilla luciferase activity was measured after 24–48 h with the dual-luciferase reporter assay system (Promega). Firefly luciferase activity was normalized to Renilla activity.

2.12 Statistical analysis

Statistical analysis was performed by the SPSS 20 (SPSS Inc., Chicago, IL, USA). Two-tailed unpaired or paired Student's t test, ANOVA (Dunnett's or LSD post hoc test) and Pearson correlation coefficients were used according to the type of experiment. Kaplan-Meier method was used to estimate survival curves, which were compared using the Log-rank (Mantel-Cox) test. The statistical significance between data sets was expressed as P values, and $P < 0.05$ was considered significant; * ($p < 0.05$), ** ($p < 0.01$), *** ($p < 0.001$).

3. Results

3.1 MIR497HG and MIR497HG-derived miR-497 and miR-195 were downregulated in BCa

MIR497HG is the host gene of the miR-497 ~ 195 cluster on chromosome 17 (Fig. 1A). We first examined the expression of MIR497HG, miR-497 and miR-195. The qRT-PCR analysis confirmed the downregulation of endogenous MIR497HG, miR-497 and miR-195 expression in BCa tissues compared with normal adjacent tissues (Fig. 1B-1D). Furthermore, we analyzed The Cancer Genome Atlas (TCGA) bladder

urothelial carcinoma (BLCA) RNA sequencing data and revealed that the expression levels of miR-497 and miR-195 were inhibited in various stage of BCa (Fig. 1E and 1F); and these data also showed that MIR497HG was downregulated in BCa (Fig. 1G). Similarly, the expression levels of MIR497HG, miR-195 and miR-497 were repressed in different BCa cell lines including 5637, T24, UMUC-3, SW780, and TCCSUP. Thus, MIR497HG, miR-497 and miR-195 were downregulated in both human BCa tissues and cell lines (Fig. 1H). These data suggest that MIR497HG, miR-497 and miR-195 may involve in the progression of BCa.

3.2 MIR47HG suppressed BCa cell growth, migration and invasion in vitro

To explore the biological functions of MIR497HG, MIR497HG was overexpressed after transfection with MIR497HG overexpression plasmid. Cell Counting Kit-8 assays and colony formation assays showed that MIR497HG overexpression significantly inhibited cell proliferation in both 5637 and T24 cells (Fig, 2A-2C). BCa cells transfected with MIR497HG presented significantly reduced scratch wound healing (Fig. 2D-2E) and lower invasion abilities (Fig. 2F, G) compared with vector control.

3.3 MiR-497 and miR-195 mediate MIR497HG-induced inhibition of BCa progression

Inspiring that a major role of miRNA-host gene lncRNAs (lnc-miRHGs) is depend on their derived miRNAs [12, 13, 30, 31], we test whether the phenotypes associated with MIR497HG are mediated by miR-497 and miR-195 in BCa cell lines. miR-497 and miR-195 inhibitor were transiently transfected into MIR497HG overexpressing 5637 and T24 cell lines. As shown in Fig. 3, miR-497 or miR-195 inhibitor partially reversed the inhibition of cell proliferation (Fig. 3A, B), migration (Fig. 3C, D), and invasion (Fig. 3E, F) induced by MIR497HG overexpression. Collectively, these data suggested that miR-497 and miR-195 are indispensable in the biological function of MIR497HG in BCa.

3.4 MiR-497 and miR-195 directly suppressed multiple key components in Hippo/Yap and TGF-β signaling

To explore the molecular pathways of miR-195 and miR-497 in BCa cells, we performed *in silico* analyses using mirPath v.3 and TargetScan. Based on the KEGG pathway enrichment analysis, 14 pathways were enriched in miR-195/497 cluster putative targets (Fig. 4A and supplementary Table S2). Then, we focused on genes predicted as miR-195/497 cluster targets and involved in hippo signaling and TGF-β pathway. Analyses of TargetScan database and previous studies [16, 17, 32, 33] revealed that 3’ UTRs of YAP, SMAD3, CCND1 and BIRC5 contained at least one conserved binding site for miR-497 ~ 195 cluster (Fig. 4B). These genes are the key components in the hippo signaling and TGF-β pathway. Next, luciferase reporter assays confirmed that miR-497 and miR-195 directly target the 3’ UTR of these candidates (Fig. 4C). The qRT-PCR and western blot analysis showed that miR-497 or miR-195 mimics

dramatically inhibited Yap, Smad3, Ccnd1 and Birc5 expression in BCa 5637 cells (Fig. 4D and supplementary Fig. S1).

3.5 MiR-497 and miR-195 coordinately attenuated Yap and Smad3 dependent transcriptional activity

Previous studies suggest that YAP–Smad3 interaction is essential for the crosstalk between hippo signaling and TGF-β pathway [34–36]. To examine whether miR-497 ~ 195 clusters affect the formation of YAP–Smad complex, we preformed immunoprecipitations to detect YAP–Smad3 interaction in 5637 cell lines. Our results showed that the interaction between YAP and Smad3 was inhibited/enhanced via miR-497 or miR-195 mimic/inhibitor treatment, respectively (Fig. 5A-5B). Interaction between Yap and Smad3 is required to positively regulate transcriptional activity of their common downstream genes including connective tissue growth factor (CTGF), a critically oncogenic target [34]. Next, CTGF luciferase assays showed that miR-497 ~ 195 clusters blocked CTGF promoter transcriptional activity mediated by Yap and Smad3 (Fig. 5C). CTGF protein expression was decreased with miR-497 or miR-195 overexpression (Fig. 5D). These data suggest that miR-497 and miR-195 synergistically repress Yap and Smad3 mediated transcriptional activity of CTGF.

3.6 E2F4 transcriptionally repressed MIR497HG expression in BCa cells

To determine the mechanism of downregulation of miR-497 ~ 195 clusters in BCa, we analyzed the host gene MIR497HG promoter sequence using MethPrimer and JASPAR. Firstly, no CpG island exists in the promoter region of MIR497HG predicted by MethPrimer. It suggested that MIR497HG expression might not repressed by promoter methylation. Then we identified conserved DNA binding sites for fork head/winged helix transcription factors. Among these transcription factors, we focused on E2F transcription factor 4 (E2F4), which was negatively correlated with MIR497HG expression (Fig. 6A) and had relatively high scores (supplementary Table S3). Therefore, we individually knocked down E2F4 or E2F6 (another high score transcription factor) in 5637 cell line using siRNA and analyzed the effect of these knockdowns on MIR497HG expression. Silencing of E2F4 significantly promoted MIR497HG expression (Fig. 6B), except knock down of E2F6 (supplementary Fig. S2). It inspired us to determine whether the transcription factor E2F4 directly targets MIR497HG. Thus, we first utilized the Ensembl and JASPAR to identify forkhead/winged helix motif (GGCGGGAA) in the MIR497HG 1.5 kb promoter region and found four potential binding sites (Fig. 6C and 6D). Next, real-time PCR after ChIP confirmed that E2F4 was significantly enriched at the MIR497HG promoter (Fig. 6E). We further confirmed that E2F4 directly regulates MIR497HG expression using luciferase reporter assays. E2F4 overexpression significantly decreased the activity of the MIR497HG promoter (Fig. 6F). Sequential mutations and deletions of four binding sites revealed that forkhead/winged helix-binding site “-189~-179” was the major site for E2F4 repressing MIR100HG transcriptional activity (Fig. 6G-I). Altogether, these data clearly demonstrate that E2F4 inhibited MIR497HG transcription by directly binding to its promoter in BCa cells.

The schematic diagram of mechanism of lncRNA MIR497HG was shown in Fig. 7. E2F4 bound to the promoter of MIR497HG to inhibit the expression of MIR497HG. miR-497 and miR-195 were derived from MIR497HG and suppressed the crosstalk of YAP and SMAD3 which were key components in Hippo/Yap and TGF-β/Smad signaling. Then, the downstream of YAP/SMAD3 complex, oncogenic CTGF, was restrained to curb cell proliferation of BCa.

4. Discussion

MIR497HG is a host gene of the miR-497 and miR-195 embedded in its first intron. MIR497HG was significantly downregulated and might serve as a potential diagnostic marker in BCa [15]. MiR-495 and miR-195 were also reduced in BCa and inhibited cancer cell progression [16, 37, 38]. Consistent with these findings, we confirmed that concomitant low expression of MIR497HG, miR-497 and miR-195 occurred in BCa, and that miR-497 and miR-195 coordinately play critical anti-oncogenic roles in BCa cells. In vitro, we found that overexpression of MIR497HG significantly inhibits the viability and proliferation of BCa cells. Mechanistically, integrated in silico analyses and luciferase reporter assays revealed that miR-195/497 cluster directly targeted YAP, SMAD3, BIRC5 and CCND1, the key components in the Hippo and TGF-β pathway. Moreover, we found that miR-195/497 cluster decreased the formation of regulatory transcription complex containing YAP and Smad3, while decreasing their common target genes, such as the gene-encoding connective tissue growth factor (CTGF) [28].

Although we focused on the targets genes in the Hippo and TGF-β pathway, it is likely that other genes or pathways are changed in bladder cancer cells as a result of miR-195/497 cluster mediated post-transcriptional gene silencing. For example, miR-195/497 cluster maintained Notch activity and HIF-1α protein expression by targeting FBXW7 in endothelial cells [39]. However, we observed no similar changes of HIF-1α and FBXW7 expression after miR-195/497 mimic treatment in BCa cells (data not shown). The reasons for the disparities remain unclear. One possibility is that miRNA perform distinct genetic programs in the different cells and microenvironments in which the cells reside.

Numerous studies points toward an important role for E2F4 with reports of transcriptional stimulatory or repressive effects of E2F4 in different cell type or tissue context [40–43]. It is possible that E2F4 serves as transcriptional activator or repressor upon binding distinct transcriptional cofactors. E2F4 drives genes transcription by interacting with acetyltransferase GCN5 and the essential cofactors TRRAP [44]. Conversely, E2F4 silence target genes relying on its interaction with the “pocket protein”, such as retinoblastoma (Rb), p107, and p130 that recruit DNMTs [40, 45]. Our data showed that E2F4 repress MIR497HG transcriptional activity, while inhibiting its embedded miR-497 and miR-195 expression. Further studies are needed to investigate whether a novel corepressor that interacts with E2F4 exists.

In conclusion, E2F4 suppressed the expression of MIR497HG, and MIR497HG suppresses bladder cancer progression through disrupting the crosstalk between Hippo/Yap and TGF-β/Smad signaling by reducing expression of four key genes involved in the these two pathways and YAP–Smad3 interaction. Our findings may open up avenues for developing effective therapeutic strategies to treat BCa.

Declarations

Ethics approval and consent to participate

The experimental protocol was established, according to the ethical guidelines of the Helsinki Declaration and was approved by the Human Ethics Committee of the Ethics Committee of Shenzhen University Nanshan Hospital. Written informed consent was obtained from individual or guardian participants.

Consent for publication

All authors agree to publish.

Availability of data and material

All data generated or analysed during this study are included in this published article.

Competing interests

All authors declare no competing interests.

Funding

This research was supported by the ‘San-ming’ Project of Medicine in Shenzhen (SZSM201612066).

Authors’ contributions

Chengle Zhuang, Changshui Zhuang and Ying Liu conceived the project, designed and performed the research; Changshui Zhuang, Chaobo Yuan, Shengqiang Fu and Weifeng Yang analyzed data; Ying Liu wrote the paper; Weifeng Yang, Jingwen Luo provided assistance in some experiments and reviewing of the manuscript.

Acknowledgments

The authors thank all the donors whose names were not included in the author list, but who participated in this program.

References

1. Sanli O, Dobruch J, Knowles MA, Burger M, Alemozaffar M, Nielsen ME, et al. Bladder cancer. Nature reviews Disease primers. 2017;3:17022.
2. Robertson AG, Kim J, Al-Ahmadie H, Bellmunt J, Guo G, Cherniack AD, et al. Comprehensive Molecular Characterization of Muscle-Invasive Bladder Cancer. Cell. 2018;174:1033.
3. Burger M, Catto JW, Dalbagni G, Grossman HB, Herr H, Karakiewicz P, et al. Epidemiology and risk factors of urothelial bladder cancer. European urology. 2013;63:234–41.

4. Felsenstein KM, Theodorescu D. Precision medicine for urothelial bladder cancer: update on tumour genomics and immunotherapy. Nature reviews Urology. 2018;15:92–111.
5. Guo G, Sun X, Chen C, Wu S, Huang P, Li Z, et al. Whole-genome and whole-exome sequencing of bladder cancer identifies frequent alterations in genes involved in sister chromatid cohesion and segregation. Nat Genet. 2013;45:1459–63.
6. Kamoun A, de Reynies A, Allory Y, Sjodahl G, Robertson AG, Seiler R, et al. A Consensus Molecular Classification of Muscle-invasive Bladder Cancer. European urology. 2020;77:420–33.
7. Spitale RC, Tsai MC, Chang HY. RNA templating the epigenome: long noncoding RNAs as molecular scaffolds. Epigenetics. 2011;6:539–43.
8. Ameres SL, Zamore PD. Diversifying microRNA sequence and function. Nature reviews Molecular cell biology. 2013;14:475–88.
9. Cai X, Cullen BR. The imprinted H19 noncoding RNA is a primary microRNA precursor. RNA. 2007;13:313–6.
10. Dhir A, Dhir S, Proudfoot NJ, Jopling CL. Microprocessor mediates transcriptional termination of long noncoding RNA transcripts hosting microRNAs. Nat Struct Mol Biol. 2015;22:319–27.
11. Rodriguez A, Griffiths-Jones S, Ashurst JL, Bradley A. Identification of mammalian microRNA host genes and transcription units. Genome research. 2004;14:1902–10.
12. Lu Y, Zhao X, Liu Q, Li C, Graves-Deal R, Cao Z, et al. lncRNA MIR100HG-derived miR-100 and miR-125b mediate cetuximab resistance via Wnt/beta-catenin signaling. Nature medicine. 2017;23:1331–41.
13. Keniry A, Oxley D, Monnier P, Kyba M, Dandolo L, Smits G, et al. The H19 lincRNA is a developmental reservoir of miR-675 that suppresses growth and Igf1r. Nat Cell Biol. 2012;14:659–65.
14. Mirzamohammadi F, Kozlova A, Papaioannou G, Paltrinieri E, Ayturk UM, Kobayashi T. Distinct molecular pathways mediate Mycn and Myc-regulated miR-17-92 microRNA action in Feingold syndrome mouse models. Nature communications. 2018;9:1352.
15. Eissa S, Safwat M, Matboli M, Zaghloul A, El-Sawalhi M, Shaheen A. (2019). Measurement of Urinary Level of a Specific Competing endogenous RNA network (FOS and RCAN mRNA/ miR-324-5p, miR-4738-3p, /lncRNA miR-497-HG) Enables Diagnosis of Bladder Cancer. *Urologic oncology* **37**: 292 e219-292 e227.
16. Itesako T, Seki N, Yoshino H, Chiyomaru T, Yamasaki T, Hidaka H, et al. The microRNA expression signature of bladder cancer by deep sequencing: the functional significance of the miR-195/497 cluster. PloS one. 2014;9:e84311.
17. Li D, Zhao Y, Liu C, Chen X, Qi Y, Jiang Y, et al. Analysis of MiR-195 and MiR-497 expression, regulation and role in breast cancer. Clinical cancer research: an official journal of the American Association for Cancer Research. 2011;17:1722–30.
18. Chae DK, Park J, Cho M, Ban E, Jang M, Yoo YS, et al. MiR-195 and miR-497 suppress tumorigenesis in lung cancer by inhibiting SMURF2-induced TGF-β receptor I ubiquitination. Molecular oncology. 2019;13:2663–78.

19. Guo ST, Jiang CC, Wang GP, Li YP, Wang CY, Guo XY, et al. MicroRNA-497 targets insulin-like growth factor 1 receptor and has a tumour suppressive role in human colorectal cancer. Oncogene. 2013;32:1910–20.
20. Furuta M, Kozaki K, Tanimoto K, Tanaka S, Arii S, Shimamura T, et al. The tumor-suppressive miR-497-195 cluster targets multiple cell-cycle regulators in hepatocellular carcinoma. PloS one. 2013;8:e60155.
21. Abbosh PH, McConkey DJ, Plimack ER. Targeting Signaling Transduction Pathways in Bladder Cancer. Current oncology reports. 2015;17:58.
22. Xia J, Zeng M, Zhu H, Chen X, Weng Z, Li S. Emerging role of Hippo signalling pathway in bladder cancer. J Cell Mol Med. 2018;22:4–15.
23. Mo JS, Park HW, Guan KL. The Hippo signaling pathway in stem cell biology and cancer. EMBO Rep. 2014;15:642–56.
24. Ciamporcero E, Shen H, Ramakrishnan S, Yu Ku S, Chintala S, Shen L, et al. YAP activation protects urothelial cell carcinoma from treatment-induced DNA damage. Oncogene. 2016;35:1541–53.
25. Liu JY, Li YH, Lin HX, Liao YJ, Mai SJ, Liu ZW, et al. Overexpression of YAP 1 contributes to progressive features and poor prognosis of human urothelial carcinoma of the bladder. BMC Cancer. 2013;13:349.
26. Massagué J. TGFβ signalling in context. Nature reviews Molecular cell biology. 2012;13:616–30.
27. Dong H, Diao H, Zhao Y, Xu H, Pei S, Gao J, et al. Overexpression of matrix metalloproteinase-9 in breast cancer cell lines remarkably increases the cell malignancy largely via activation of transforming growth factor beta/SMAD signalling. Cell proliferation. 2019;52:e12633.
28. Luo K. (2017). Signaling Cross Talk between TGF-beta/Smad and Other Signaling Pathways. *Cold Spring Harbor perspectives in biology* 9.
29. Zhao B, Ye X, Yu J, Li L, Li W, Li S, et al. TEAD mediates YAP-dependent gene induction and growth control. Genes Dev. 2008;22:1962–71.
30. Wu X, Wang Y, Yu T, Nie E, Hu Q, Wu W, et al. Blocking MIR155HG/miR-155 axis inhibits mesenchymal transition in glioma. Neurooncology. 2017;19:1195–205.
31. Augoff K, McCue B, Plow EF, Sossey-Alaoui K. miR-31 and its host gene lncRNA LOC554202 are regulated by promoter hypermethylation in triple-negative breast cancer. Mol Cancer. 2012;11:5.
32. Zhang L, Yu Z, Xian Y, Lin X. microRNA-497 inhibits cell proliferation and induces apoptosis by targeting YAP1 in human hepatocellular carcinoma. FEBS open bio. 2016;6:155–64.
33. Jafarzadeh M, Soltani BM, Dokanehiifard S, Kay M, Aghdami N, Hosseinkhani S. Experimental evidences for hsa-miR-497-5p as a negative regulator of SMAD3 gene expression. Gene. 2016;586:216–21.
34. Fujii M, Toyoda T, Nakanishi H, Yatabe Y, Sato A, Matsudaira Y, et al. TGF-β synergizes with defects in the Hippo pathway to stimulate human malignant mesothelioma growth. The Journal of experimental medicine. 2012;209:479–94.

35. Luo K. (2017). Signaling Cross Talk between TGF-β/Smad and Other Signaling Pathways. *Cold Spring Harbor perspectives in biology* 9.
36. Varelas X, Sakuma R, Samavarchi-Tehrani P, Peerani R, Rao BM, Dembowy J, et al. TAZ controls Smad nucleocytoplasmic shuttling and regulates human embryonic stem-cell self-renewal. Nat Cell Biol. 2008;10:837–48.
37. Han Y, Chen J, Zhao X, Liang C, Wang Y, Sun L, et al. MicroRNA expression signatures of bladder cancer revealed by deep sequencing. PloS one. 2011;6:e18286.
38. Zhang Y, Zhang Z, Li Z, Gong D, Zhan B, Man X, et al. MicroRNA-497 inhibits the proliferation, migration and invasion of human bladder transitional cell carcinoma cells by targeting E2F3. Oncol Rep. 2016;36:1293–300.
39. Yang M, Li CJ, Sun X, Guo Q, Xiao Y, Su T, et al. MiR-497∼195 cluster regulates angiogenesis during coupling with osteogenesis by maintaining endothelial Notch and HIF-1α activity. Nature communications. 2017;8:16003.
40. López-Díaz FJ, Gascard P, Balakrishnan SK, Zhao J, Del Rincon SV, Spruck C, et al. Coordinate transcriptional and translational repression of p53 by TGF-β1 impairs the stress response. Molecular cell. 2013;50:552–64.
41. Kanakkanthara A, Huntoon CJ, Hou X, Zhang M, Heinzen EP, O'Brien DR, et al. ZC3H18 specifically binds and activates the BRCA1 promoter to facilitate homologous recombination in ovarian cancer. Nature communications. 2019;10:4632.
42. Cuitiño MC, Pécot T, Sun D, Kladney R, Okano-Uchida T, Shinde N, et al (2019). Two Distinct E2F Transcriptional Modules Drive Cell Cycles and Differentiation. *Cell reports* **27**: 3547–3560 e3545.
43. Hsu J, Arand J, Chaikovsky A, Mooney NA, Demeter J, Brison CM, et al. E2F4 regulates transcriptional activation in mouse embryonic stem cells independently of the RB family. Nature communications. 2019;10:2939.
44. Lang SE, McMahon SB, Cole MD, Hearing P. E2F transcriptional activation requires TRRAP and GCN5 cofactors. J Biol Chem. 2001;276:32627–34.
45. Iaquinta PJ, Lees JA. Life and death decisions by the E2F transcription factors. Curr Opin Cell Biol. 2007;19:649–57.

Figures

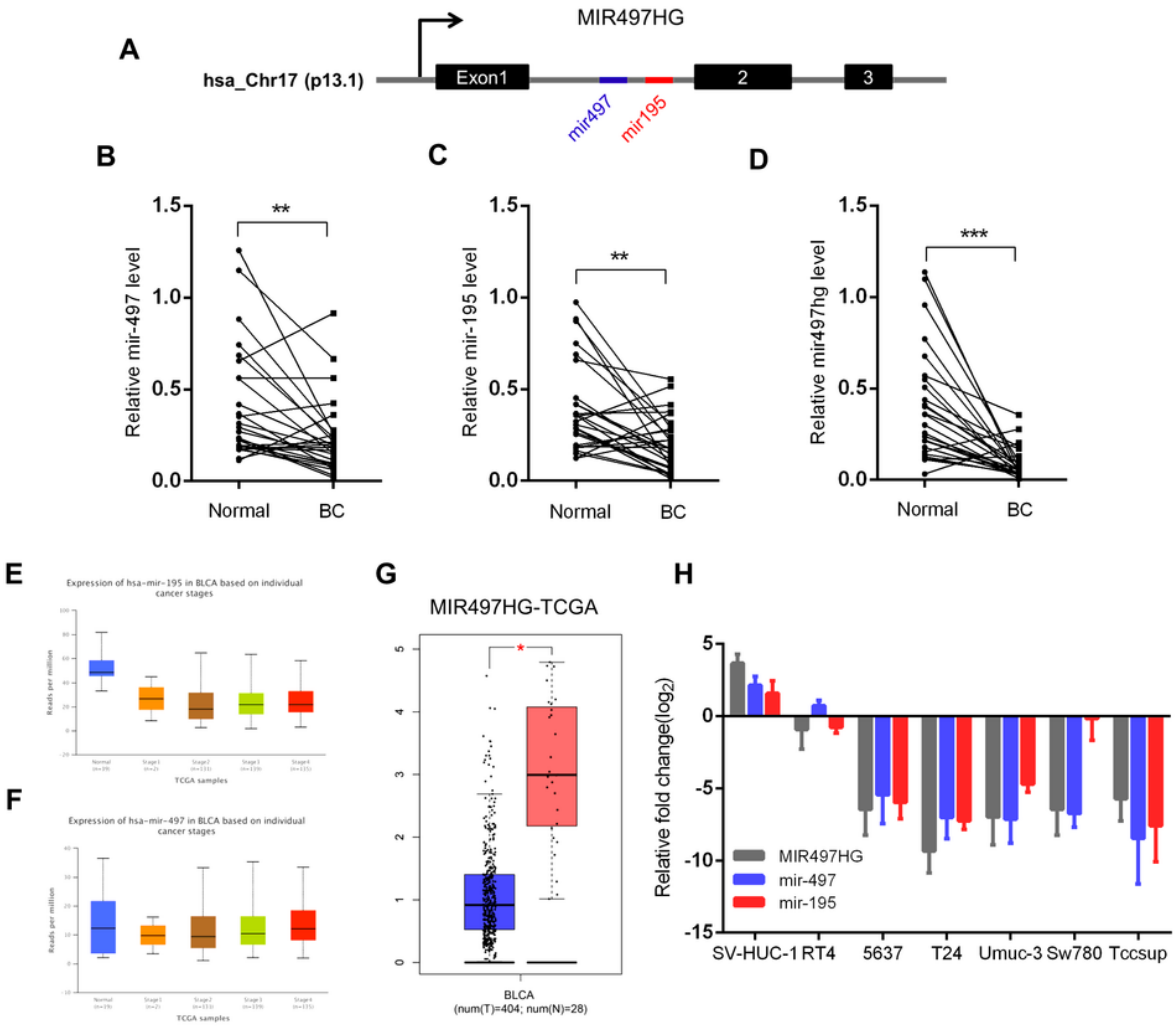

Figure 1

MIR497HG and embedded miR-497 and miR-195 were downregulated in bladder cancer. (A) Genomic representation of MIR497HG, host gene of the miR-497/195 cluster, was shown on human chromosome 17. (B-D) The expression of MIR497HG and miR-497/195 cluster analyzed by qRT-PCR in 27 paired BCa tissues and adjacent normal tissues. **P < 0.01 and ***P < 0.001 by paired-samples T test. (E-G) TGCA bladder cancer datasets were analyzed for MIR497HG and miR-497/195 cluster expression. *P <0.05. (H) The qRT-PCR analysis of MIR497HG, miR-497 and miR-195 expression levels among a panel of 7 BCa cell lines. GAPDH or U6 snRNA served as the internal control.

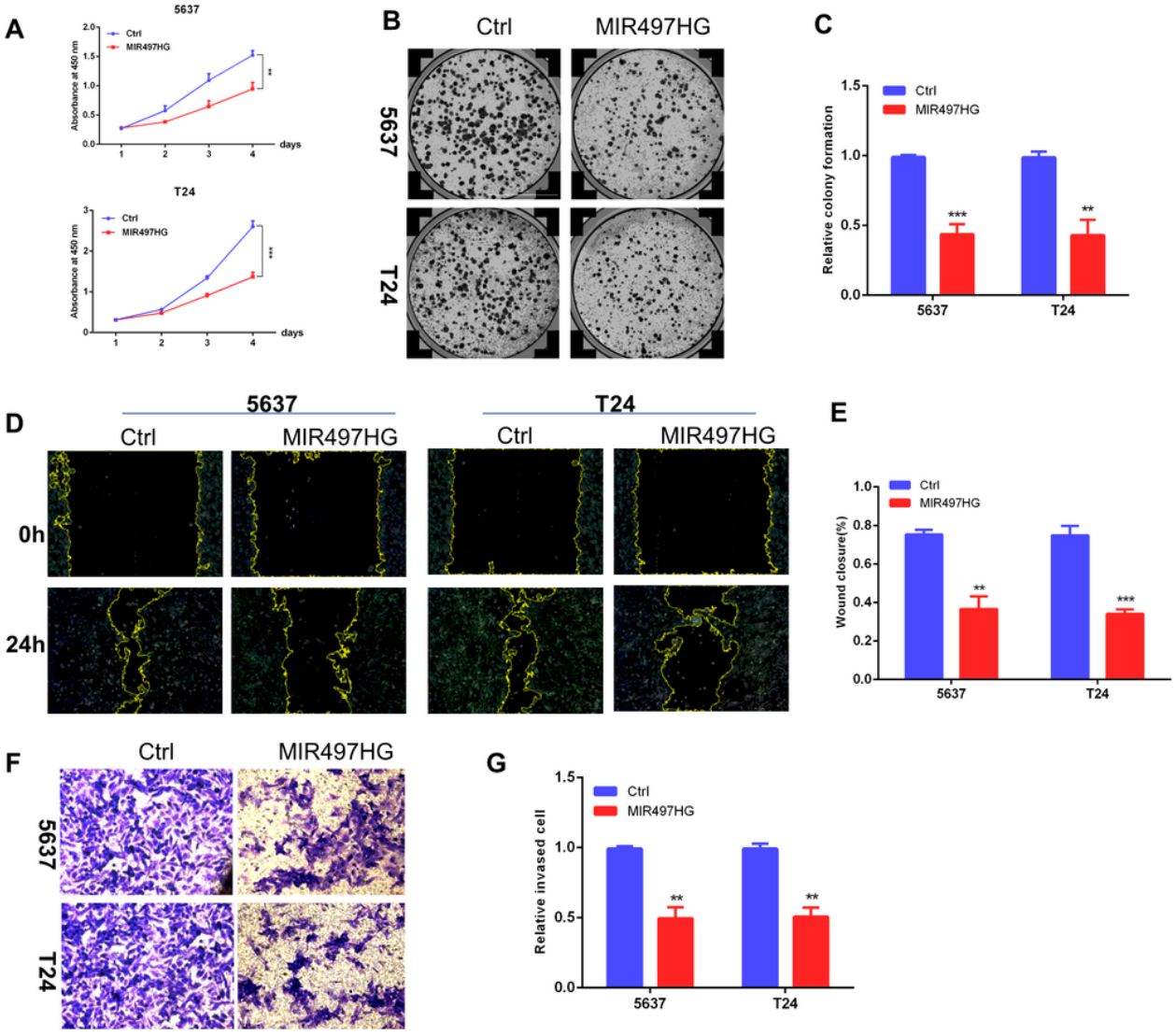

Figure 2

MIR47HG suppresses BCa cell growth, migration and invasion in vitro. (A) The CCK-8 assay showed that overexpression of MIR497HG repressed BCa cell proliferation in 5637 and T24 cells. **P < 0.01, ***P < 0.001 by independent-samples T test in each time point. (B, C) Colony formation assays of 5637 (C) and T24 (D) cells treated with MIR497HG overexpression vector. **P <0.01 by independent-samples T test. Error bars indicate means ± SD, n = 3 for technical replicates. (D, E) 5637 and T24 cell migraion was suppressed significantly by MIR497HG. (F, G) Cell invasion of 5637 and T24 cells was inhibited obviously via overexpression of MIR497HG.

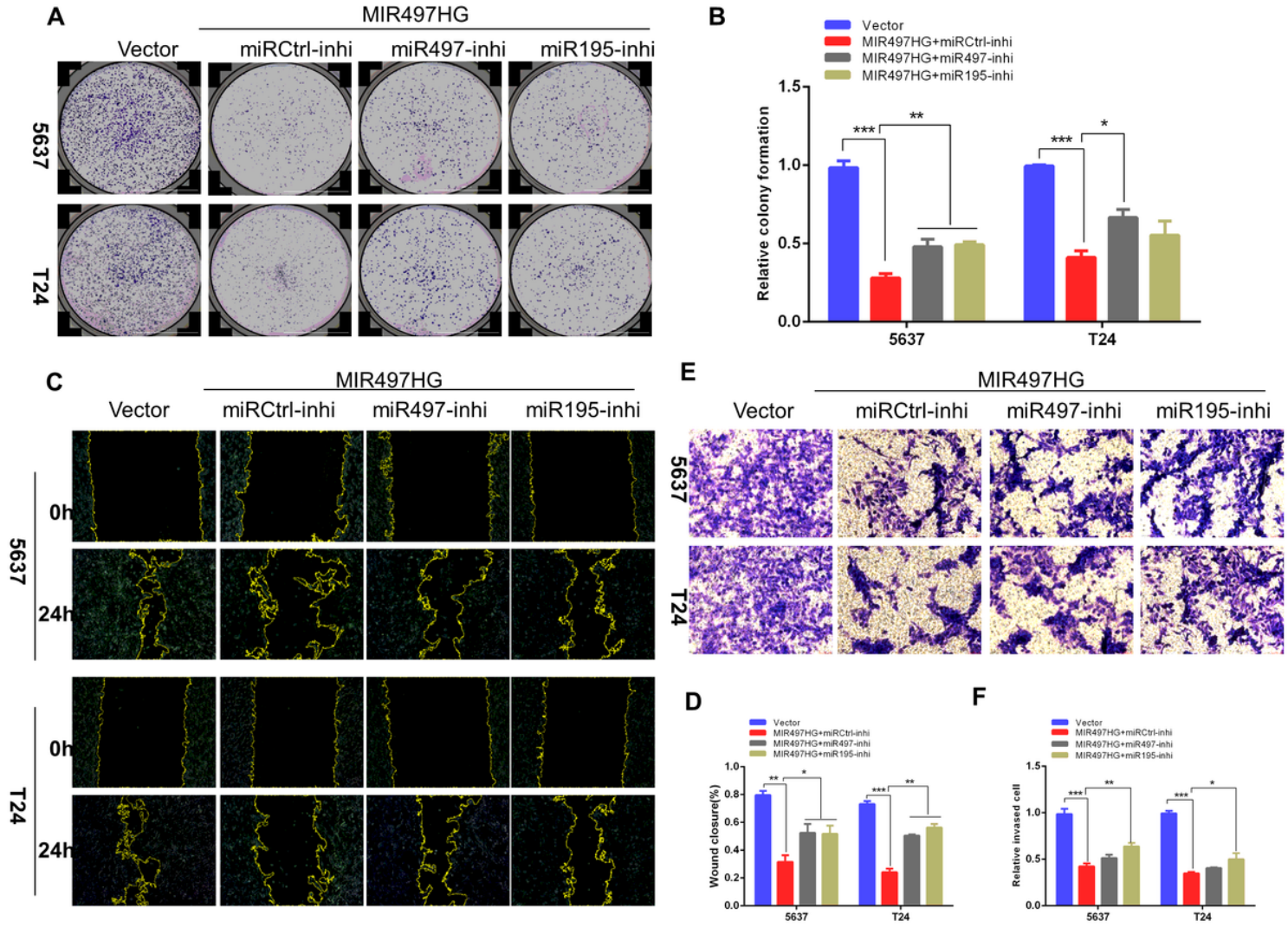

Figure 3

MiR-497 and miR-195 mediate MIR497HG-induced inhibition of BCa progression. (A, B) MiR-497 or miR-195 inhibitor rescued partial MIR497HG-induced inhibition of BCa cell proliferation significantly. (C-F) The inhibitory effects of MIR497HG on cell migration or invasion were partial reduced by miR-497 or miR-195 inhibitor. *P<0.05, **P < 0.01, ***P < 0.001.

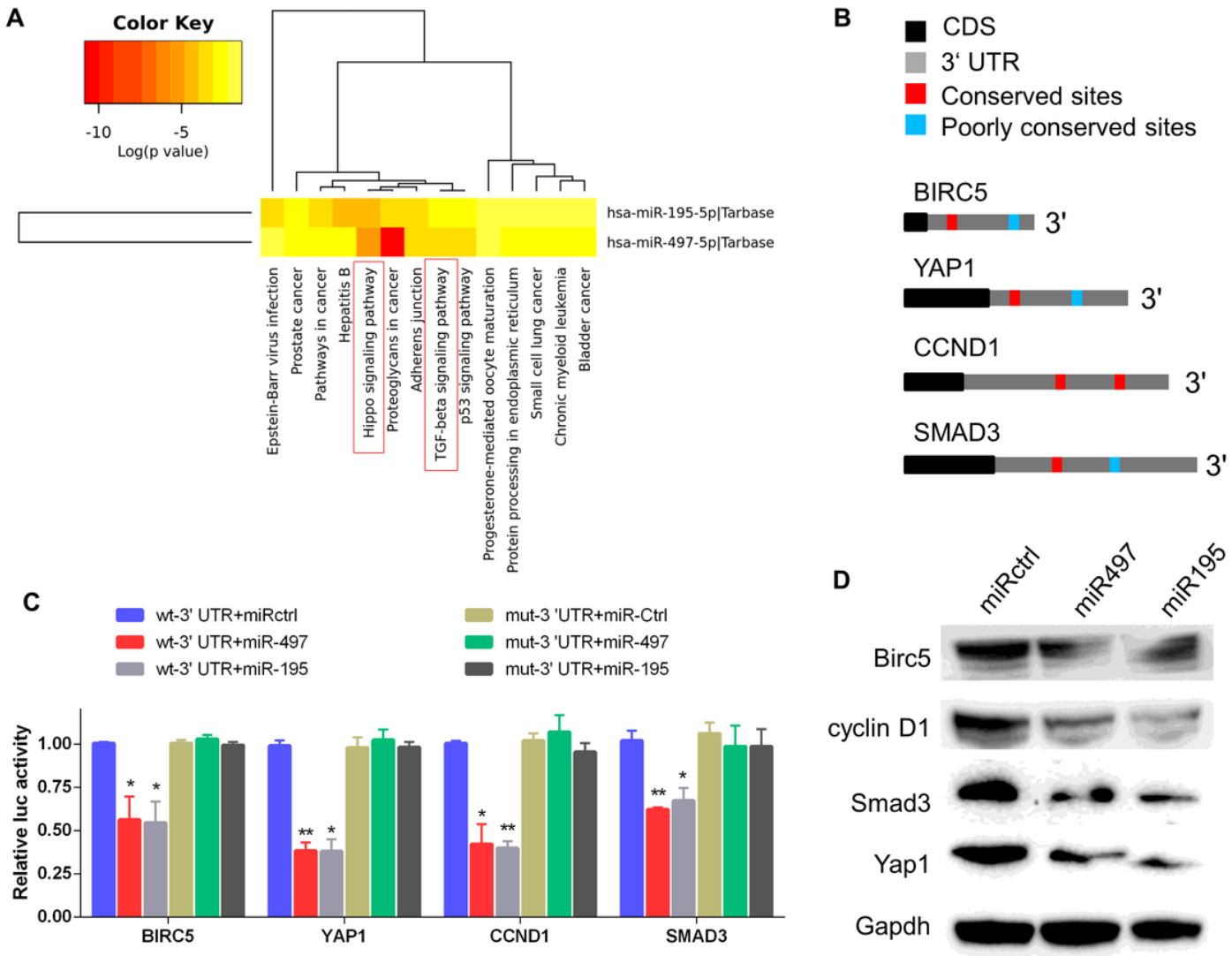

Figure 4

MiR-497 and miR-195 directly suppressed multiple key components in Hippo/Yap and TGF-β signaling. (A) The KEGG analysis of miR-497 and miR-195 target genes. (B) Predicted miR-497 and miR-195 binding conversed (red) and poorly conversed (blue) sites in 3' UTRs of Birc5, Yap1, CCND1 and Smad3. CDS, coding sequence. (C) Luciferase reporter assay of candidates predicted to be regulated by miR-497 or miR-195. Renilla luciferase activity was normalized to firefly activity. n = 3 independent experiments. *P < 0.01 and **P < 0.01 by Student's t test. (D) Western blot analysis of Birc5, cyclin D1, Smad3 and Yap1 in the indicated cells. Gapdh served as the loading control. Representative of three independent experiments.

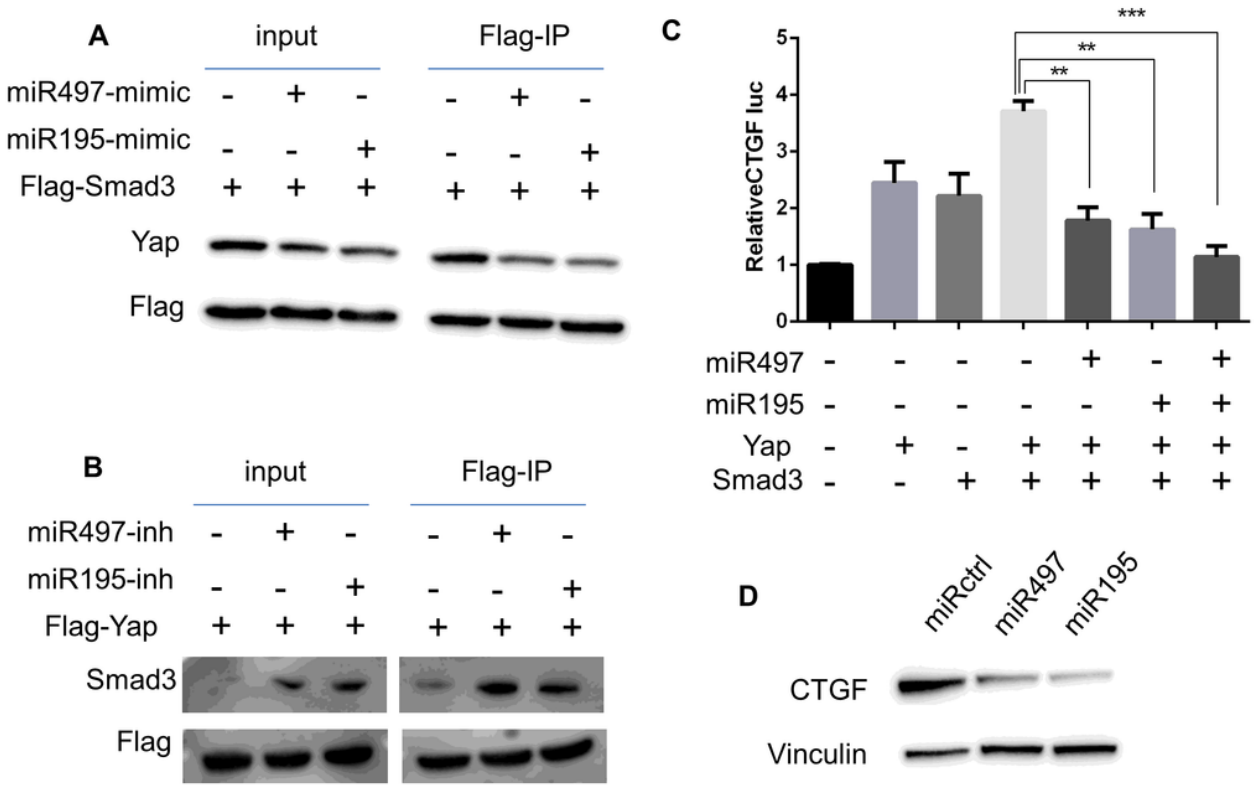

Figure 5

MiR-497 and miR-195 coordinately attenuated Yap and Smad3 dependent transcriptional activity. (A-B) 5637 cells were transfected with expression vectors as indicated. Cell lysates were subjected to immunoprecipitation (IP) with an anti-Flag antibodyand subsequent WB with indicated antibodies. (C) CTGF-luciferase reporter was co-transfected with other plasmids into 5637 cells as indicated for luciferase assay. Results are expressed as mean ± SD. **P < 0.01 and ***P < 0.001. (D) Western blot analysis of CTGF in the cells transfected with miR-497 and miR-195 mimics.

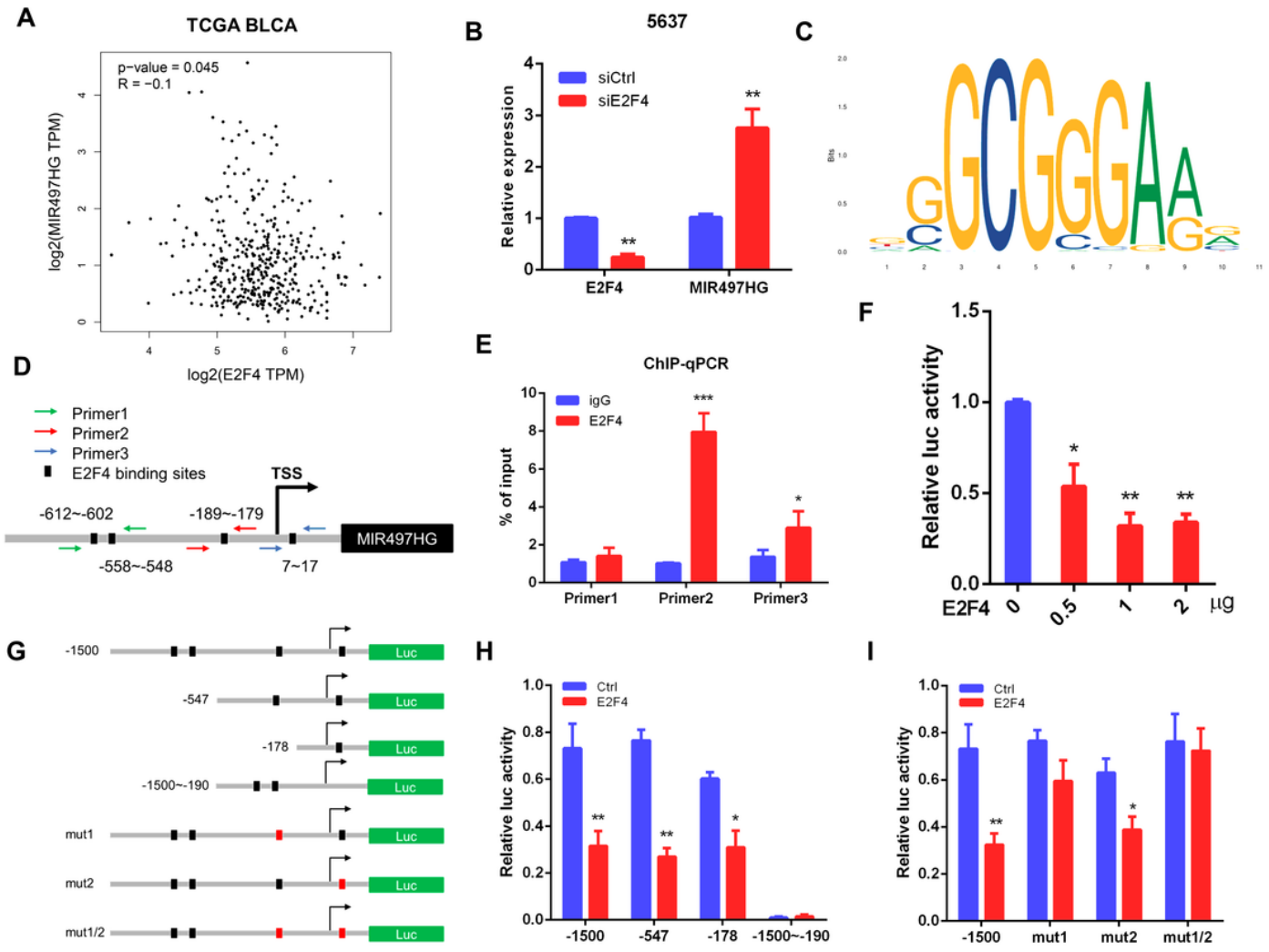

Figure 6

E2F4 transcriptionally repressed MIR497HG expression in BCa cells. (A) The correlation between E2F4 gene expression and MIR497HG level in TGCA datasets. (B) 5637 cells expressing either E2F4 or non-silencing control siRNA were analyzed for E2F4 (left) or MIR497HG (right) mRNA expression using qRT-PCR. (C) E2F4-binding motif. (D) E2F4 binding in the MIR497HG promoter and primer designation. (E) Chromatin immunoprecipitation was performed in 5637 cells with either IgG or E2F4 and subsequently subjected to qPCR analysis with the indicated primers. Student's t test, *p < 0.05 and ***p < 0.001. (F) Hif-1a promoter activity was determined in 5637 with E2F4 overexpression. One-way ANOVA with Dunnett's post-test, *p < 0.05 and **p < 0.01. (G) A schematic representation of deletion or mutation constructs spanning the −1,500 to +200 region of the MIR497HG promoter. (H-I) The luciferase vector pGL3 driven by either wild-type, deletion or mutant MIR497 promoter was transfected in 5637 cells, and luciferase activity was measured. n = 3 independent experiments. *P < 0.05, **P < 0.01 by Student's t test.

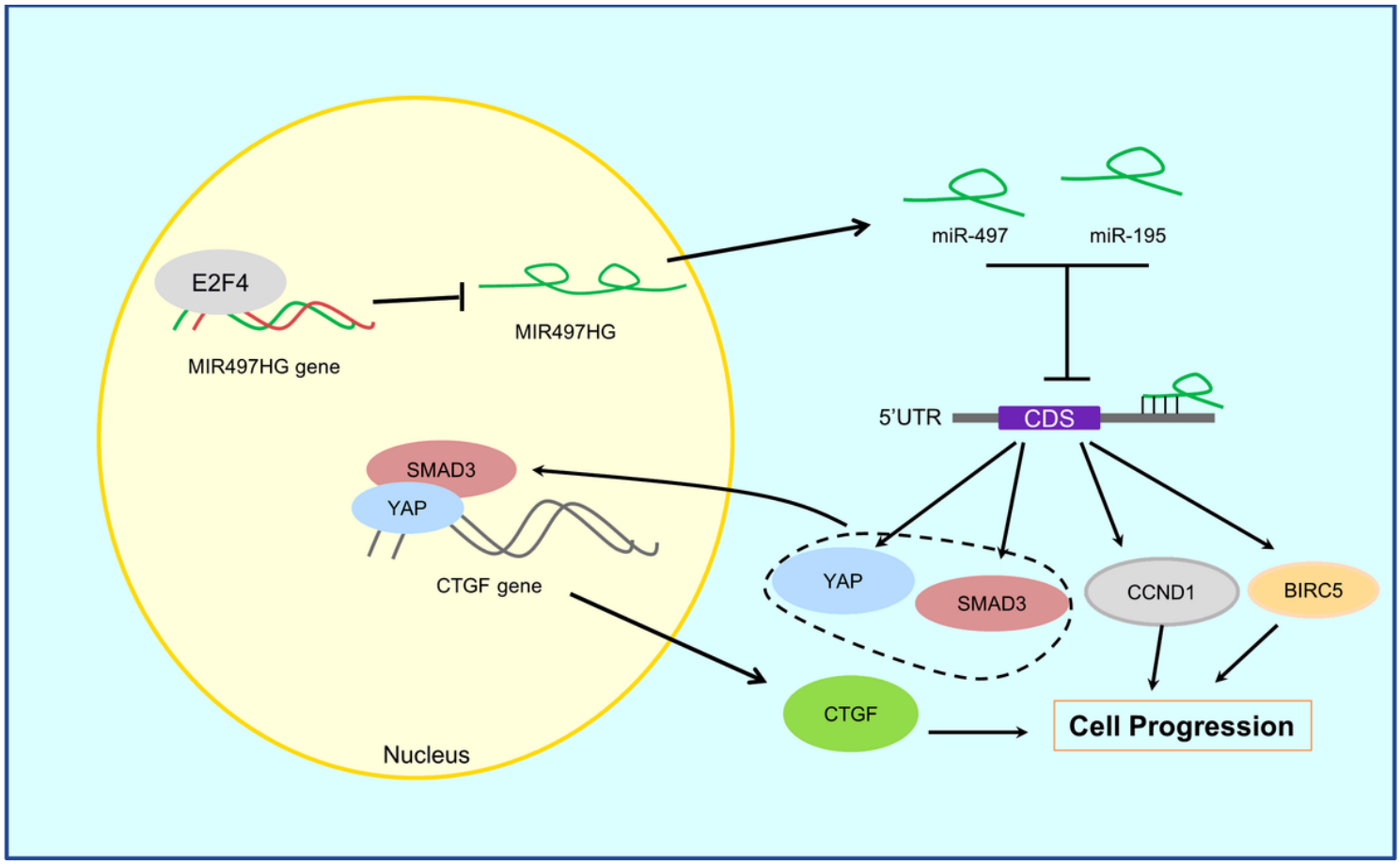

Figure 7

The schematic diagram of mechanism of lncRNA MIR497HG in BCa. E2F4 bound to the promoter of MIR497HG to act as inhibitory transcription factors to suppress the expression of MIR497HG. miR-497 and miR-195 were derived from MIR497HG and they suppressed the crosstalk of YAP and SMAD3 which were key components in Hippo/Yap and TGF-β/Smad signaling. Then, the downstream of YAP/SMAD3 complex, oncogenic CTGF, was restrained to curb cell progression of BCa.

Supplementary Files

This is a list of supplementary files associated with this preprint. Click to download.

- TableS3.xlsx
- TableS2.xlsx
- TableS1.docx
- FigS2.tif
- FigS1.tif